

Enhanced Deuteron Coalescence Probability in Jets

S. Acharya *et al.*^{*}
(ALICE Collaboration)



(Received 26 January 2023; revised 7 April 2023; accepted 5 June 2023; published 26 July 2023)

The transverse-momentum (p_T) spectra and coalescence parameters B_2 of (anti)deuterons are measured in p-p collisions at $\sqrt{s} = 13$ TeV for the first time in and out of jets. In this measurement, the direction of the leading particle with the highest p_T in the event ($p_T^{\text{lead}} > 5$ GeV/c) is used as an approximation for the jet axis. The event is consequently divided into three azimuthal regions, and the jet signal is obtained as the difference between the toward region, that contains jet fragmentation products in addition to the underlying event (UE), and the transverse region, which is dominated by the UE. The coalescence parameter in the jet is found to be approximately a factor of 10 larger than that in the underlying event. This experimental observation is consistent with the coalescence picture and can be attributed to the smaller average phase-space distance between nucleons in the jet cone as compared with the underlying event. The results presented in this Letter are compared to predictions from a simple nucleon coalescence model, where the phase-space distributions of nucleons are generated using PYTHIA8 with the Monash 2013 tuning, and to predictions from a deuteron production model based on ordinary nuclear reactions with parametrized energy-dependent cross sections tuned on data. The latter model is implemented in PYTHIA8.3. Both models reproduce the observed large difference between in-jet and out-of-jet coalescence parameters, although the almost flat trend of the B_2^{jet} is not reproduced by the models, which instead give a decreasing trend.

DOI: [10.1103/PhysRevLett.131.042301](https://doi.org/10.1103/PhysRevLett.131.042301)

The production mechanisms of light (anti)nuclei in high-energy hadronic collisions is still unclear and currently under intense debate in the scientific community, despite the plethora of results published in recent years at different collision energies, ranging from the AGS [1–4], to the SPS [5], RHIC [6–11], and the LHC [12–27]. The experimental data are typically described using two different phenomenological approaches: the baryon coalescence approach and the statistical hadronization model (SHM). In the coalescence model [28–34], multibaryon states are assumed to be formed by coalescence of baryons that are close in phase space at kinetic freeze-out (occurring when the elastic scatterings among the particles produced in the collision cease). In the simple coalescence approach [29], only momentum correlations are considered, while in state-of-the-art implementations [30], the quantum-mechanical properties of baryons and bound states are taken into account and the coalescence probability is calculated from the overlap between the phase-space distributions of individual (pointlike) baryons and the

Wigner density of the final-state cluster. The phase-space distributions of nucleons at freeze-out are generated using general-purpose Monte Carlo (MC) event generators or relativistic hydrodynamical simulations [31,35]. In the SHM [36–43], light (anti)nuclei, as well as other hadron species, are assumed to be emitted by a source in local thermal and hadrochemical equilibrium with their abundances being fixed at chemical freeze-out (occurring when the inelastic scatterings stop). The grand-canonical approach provides an excellent description of the measured hadron yields in central nucleus-nucleus collisions, in which a large number of particles is produced, ranging from a few hundred to 2000 charged particles per unit of rapidity with increasing collision energy [40]. For small systems, such as those produced in proton-proton (p-p) and proton-nucleus collisions, the production of light nuclei can be described using a different implementation of this model based on the canonical ensemble, where exact conservation of quantum numbers is required [43]. Significant deviations in this case are observed between the experimental data and the predictions from the canonical SHM [24]. The study of the production mechanisms of multibaryon bound states in high-energy hadronic collisions is one of the goals of the experimental program of ALICE.

Measurements of light (anti)nuclei produced at accelerators are also important for indirect dark matter (DM) searches as they provide input for the estimates of the background of antinuclei produced in space. Several

^{*}Full author list given at the end of the Letter.

Published by the American Physical Society under the terms of the [Creative Commons Attribution 4.0 International license](#). Further distribution of this work must maintain attribution to the author(s) and the published article's title, journal citation, and DOI.

experiments, such as AMS-02 [44] and GAPS [45], are searching for antinuclei [46,47], but, so far, only antiprotons have been detected in space [48]. The possible presence of antinuclei in our Galaxy could be explained either by reactions of cosmic rays (CRs) with the interstellar medium (ISM) or by decays and/or annihilations of dark matter candidates. Both CRs and the ISM mostly consist of hydrogen (90%), helium (8%), and only in small percentage of heavier nuclei [49]. Hence, most of the relevant collisions for the production of CR antinuclei in the Galaxy are p-p, p-⁴He, and ⁴He-p. Antinuclei are produced if the center-of-mass energy per nucleon–nucleon collision ($\sqrt{s_{NN}}$) of such collisions is above a given energy threshold, which is 6 GeV for antideuterons and 8 GeV for anti-³He, for instance. Hence, one of the goals of the existing experimental programs at different accelerator facilities is to pin down the microscopic production process of antinuclei in hadronic collisions or DM decay, in order to be able to correctly interpret the future measurements in space.

Further insight into the (anti)nuclei production mechanisms can be obtained by measuring their production in and out of jets in p-p collisions. Hadrons in the jet cone are closer in phase space compared with hadrons out of the jet. In a jet fragmentation, the produced particles are strongly correlated in phase space, i.e., particles which are close in space have also similar momenta [50,51]. In the coalescence picture, this condition should result in a larger coalescence probability in jets compared with that out of jets, since the proximity in both space and momentum is required for coalescence. Hence, the probability of coalescence in jets is increased with respect to that in the underlying event (UE), where space and momentum are not correlated, i.e., close-by particles can have very different momenta and vice-versa. The coalescence probability can be quantified by the coalescence parameter B_A , defined, in the case of deuterons, as the ratio between the invariant yield of the deuterons and the square of the invariant yield of protons:

$$B_2 = \left(\frac{1}{2\pi p_T^d} \frac{d^2 N_d}{dy dp_T^d} \right) \Bigg/ \left(\frac{1}{2\pi p_T^p} \frac{d^2 N_p}{dy dp_T^p} \right)^2, \quad (1)$$

where the labels d and p indicate the deuteron and the proton, respectively, and $p_T^p = p_T^d/2$, assuming that protons and neutrons have the same production spectra, since they belong to the same isospin doublet.

Deuteron production in jets has already been measured in p-p collisions at $\sqrt{s} = 13$ TeV by the ALICE Collaboration using the two-particle correlation method [22]. The p_T spectrum of (anti)deuterons in the jet is found to be consistent with predictions based on the PYTHIA8 event generator [52] coupled to a simple coalescence afterburner, as shown in Ref. [53]. In the latter, deuteron formation is assumed to happen if a proton and a neutron have a momentum difference $\Delta p < p_0$, with $p_0 = 110$ MeV/ c ,

thus ignoring the space coordinates in the calculation of the coalescence probability. It was also concluded that the yield of deuterons in jets, in events with a leading particle with $p_T > 5$ GeV/ c at midrapidity, is about 10% of that in the UE.

This study is expanded in this Letter and complemented by the first measurement of (anti)deuteron coalescence parameters in and out of jets. The direction of a leading particle with high transverse momentum ($p_T^{\text{lead}} > 5$ GeV/ c) at midrapidity is used as an approximation for the jet axis. The p_T spectra and coalescence parameters of (anti)deuterons are measured in three different azimuthal regions defined based on $\Delta\varphi = |\varphi_d - \varphi_{\text{lead}}|$, where φ_d is the azimuthal angle of the deuterons and φ_{lead} is that of the leading particle. The three 120°-wide azimuthal regions and the corresponding $\Delta\varphi$ intervals are the same as those defined in Refs. [54,55]: the one around the leading particle (toward, $|\Delta\varphi| < 60^\circ$), the one back-to-back to it (away, $|\Delta\varphi| > 120^\circ$), and the one transverse to both of them (transverse, $60^\circ < |\Delta\varphi| < 120^\circ$). The toward and away regions contain contributions from the leading and recoil jets in addition to the underlying event, while the transverse region is dominated by the underlying event.

A detailed description of the ALICE apparatus and its performance can be found in Refs. [56] and [57]. Trajectories of charged particles are reconstructed in the ALICE central barrel with the inner tracking system (ITS) [56] and the time projection chamber (TPC) [58], which cover the full azimuthal angle and the pseudorapidity interval $|\eta| < 0.9$. These are located within a large solenoidal magnet, providing a highly homogeneous magnetic field of 0.5 T parallel to the beam line. The TPC provides up to 159 spatial points per track for charged-particle reconstruction and particle identification (PID) through the measurement of the specific ionization energy loss dE/dx in the gas volume. The PID is complemented by the time-of-flight (TOF) system [59] located at a radial distance of 3.7 m from the nominal interaction point. It measures the arrival time of particles relative to the event collision time provided by the TOF detector itself or by the T0 detectors, two arrays of Cherenkov counters located at forward and backward rapidities ($4.6 < \eta < 4.9$ and $-3.3 < \eta < -3.0$) [57,60].

The data used for this analysis were collected in 2016, 2017, and 2018 during the LHC p-p runs at $\sqrt{s} = 13$ TeV. A minimum bias (MB) event trigger was used, which requires coincident signals in the V0 detectors (two plastic scintillator arrays located at forward and backward rapidities, $2.8 < \eta < 5.1$ and $-3.7 < \eta < -1.7$ [61]) synchronous with the bunch crossing time defined by the LHC clock. Events with multiple collision vertices, reconstructed from track segments in the two innermost layers of the ITS, are tagged as pile up and removed from the analysis [57]. A total of approximately 1.7 billion MB p-p events are considered for further analysis, corresponding to an integrated luminosity of about 30 nb^{-1} . Events with at least one charged primary

particle with $p_T > 5 \text{ GeV}/c$ are selected, which correspond to approximately 1% of the MB p-p collisions.

Deuteron candidates are selected from charged-particle tracks reconstructed in the ITS and TPC in the pseudorapidity interval $|\eta| < 0.8$. Basic track quality criteria are applied, e.g., selecting the number of space points associated to the track in the TPC and ITS and the χ^2 of the track fit, as done in previous light (anti)nucleus analyses, such as in Ref. [20]. The track selection criteria used for the leading particle are the same as in Ref. [54].

(Anti)deuterons are identified in the rapidity interval $|y| < 0.5$ in the range $0.6 < p_T < 1.2 \text{ GeV}/c$ by requiring that their energy loss per unit of track length measured by the TPC is within $3\sigma_{dE/dx}$ from the expected average for (anti)deuterons, where $\sigma_{dE/dx}$ is the dE/dx resolution. For $1.2 < p_T < 3.0 \text{ GeV}/c$, the particle identification is complemented by the TOF, and the (anti)deuteron signal is extracted from a fit to the $n\sigma_{\text{TOF}} = (\Delta t - \Delta t_d)/\sigma_{\text{TOF}}$ distribution, where Δt is the measured time of flight, Δt_d its expected value for deuterons, and σ_{TOF} the resolution on the time-of-flight measurement. The fit function consists of a Gaussian with an exponential tail on the right side for the signal and the sum of two exponential functions for the background [13]. The signal is extracted by integrating the signal function in the asymmetric interval $[\mu_0 - 3\sigma_{\text{TOF}}, \mu_0 + 3.5\sigma_{\text{TOF}}]$, where μ_0 is the mean of the Gaussian function.

The raw (anti)deuteron p_T spectra are corrected for the reconstruction efficiency and, only for deuterons, for the fraction of secondary deuterons produced by spallation in interactions between primary particles and the detector material. This correction is based on fits to the distance of closest approach (DCA) of the deuteron track to the primary vertex using template distributions extracted from MC simulations, as described in Refs. [20,21,23]. Both corrections are calculated using MC simulations in which (anti)nuclei are embedded into p-p collision events generated using PYTHIA8.1 with the Monash 2013 tune [62]. (Anti)nuclei are generated with uniform p_T and rapidity distributions within $0 < p_T < 10 \text{ GeV}/c$ and $-1 < y < 1$. The passage of particles through the ALICE detector is simulated using GEANT4 [63]. The reconstruction efficiency is calculated as the ratio of the number of reconstructed and generated (anti)deuterons in the simulation, after the proper reweighting of the generated p_T distribution according to the Lévy-Tsallis function. The same track selection and PID criteria as those used in the data are applied. The fraction of secondary deuterons is approximately 0.5 in the lowest p_T interval ($0.6 < p_T < 0.8 \text{ GeV}/c$) and decreases exponentially with increasing p_T , becoming negligible for $p_T > 1.6 \text{ GeV}/c$. The fraction of secondary deuterons is weakly dependent on the azimuthal region.

The dominant contributions to the systematic uncertainties are related to the track selection, the particle identification, the limited knowledge of the ALICE material

budget, the uncertainties on the hadronic interaction cross section of (anti)deuterons, and the procedure used to estimate the fraction of secondary nuclei. The uncertainty related to the track selection is estimated by repeating the analysis using different track selection criteria and considering the rms of the distribution of the results in each p_T interval. This contribution is found to range between 8(1)% and 6(5)% for deuterons (antideuterons), depending on p_T . Such uncertainty is larger for deuterons at low p_T , due to the DCA cut variations which are sensitive to the secondary nuclei. The PID uncertainty is estimated by varying the (anti)deuteron selection criteria in the TPC and TOF, the fit functions, and the signal extraction strategy (bin counting or integral of the fit function). The PID systematic uncertainty rises with p_T , from 4% to 8%. The systematic uncertainty due to the estimate of the primary fraction correction is obtained by varying the conditions (selection criteria, histogram bin width, fit range) of the fits to the DCA distributions used to estimate the correction factors. This contribution depends on the azimuthal region, and it ranges between 14% (10% and 7%) and a few percent for the away region (toward and transverse, respectively). The contribution from ITS-TPC and TPC-TOF matching efficiencies are estimated from charged particle tracks by comparing the probabilities of prolonging a track from the TPC to the ITS (TOF) in the data and MC [20]. The uncertainty is approximately 2% for the ITS-TPC matching efficiency and 5% for the TPC-TOF one, weakly dependent on p_T . The uncertainty on the material budget (1%) is taken from Ref. [20]. The uncertainty on the hadronic interaction cross section of (anti)deuterons is estimated by varying the default inelastic cross section of (anti)deuterons in GEANT4 by the uncertainties of the measurements [49,64–67] and is $\sim 1\%$ (3%) for deuterons (antideuterons). The total uncertainty is obtained as the quadratic sum of each individual contribution and is found to be about 10%.

The average of the deuteron and antideuteron p_T distributions measured in the three azimuthal regions discussed above, are shown in Fig. 1 left. Individual Lévy-Tsallis fits [68] are also shown. The p_T spectrum of (anti)deuterons in jets is obtained by subtracting the spectrum in the transverse region, dominated by the underlying event, from that in the toward region, which contains contributions from both jet fragmentation and the underlying event. In the subtraction, the systematic uncertainties are treated as independent, to be conservative. The resulting spectrum, with a much harder shape compared with the UE spectrum, is shown in Fig. 1 right, with squared markers, and compared to the in-jet deuteron spectrum measured with the two-particle correlation method taken from Ref. [22]. Excellent agreement is found between the deuteron p_T spectra in jets obtained with the two methods, proving the validity of the subtraction method to obtain the deuteron spectrum in jets. These results confirm that the integrated yield of deuterons in jets, in events with $p_T^{\text{lead}} > 5 \text{ GeV}/c$ at midrapidity, is only roughly 10% of that in the UE, as already pointed out in Ref. [22].

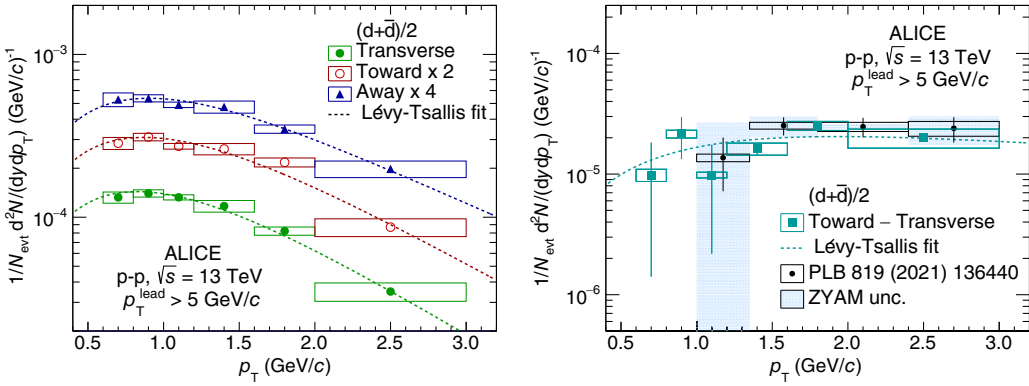


FIG. 1. Average of deuteron and antideuteron p_T -differential yields in the three azimuthal regions (on the left) and in jets (on the right), measured in p-p collisions at $\sqrt{s} = 13$ TeV. Statistical and systematic uncertainties are represented by vertical bars and boxes, respectively. On the right, shaded (blue) boxes show the uncertainty on the results from Ref. [22] related to the subtraction of the uncorrelated background using the ZYAM method [69]. Individual Lévy-Tsallis fits are also shown.

The coalescence parameters in the jet (B_2^{jet}) and underlying event (B_2^{UE}) are calculated using Eq. (1). The spectra for (anti)protons are derived from the R_T -differential p_T spectra published in Ref. [70], integrating over the full R_T , which is the underlying event activity classifier defined as $R_T = N_T^{\text{ch}} / \langle N_T^{\text{ch}} \rangle$ (N_T^{ch} being the charged-particle multiplicity measured in the transverse region and $\langle N_T^{\text{ch}} \rangle$ its average) [54]. The p_T spectrum of (anti)protons in jets is obtained by subtracting the efficiency-corrected p_T spectra in the transverse region from those in the toward region taken from Ref. [70], as done for deuterons. The coalescence parameters B_2^{jet} and B_2^{UE} are shown in Fig. 2 as a function of the transverse momentum per nucleon, p_T/A . The coalescence parameter B_2^{jet} is found to be about a factor of

10 larger than that in the underlying event, with a significance of about 21σ . Hence, despite the limited contribution of nuclei arising from jets to their total production yield, the probability that two nucleons in the jet cone coalesce into a deuteron is enhanced with respect to the corresponding coalescence probability in the underlying event. This experimental observation can be interpreted, within the coalescence model, as due to the reduced distance in phase space between nucleons in the jets compared with those in the underlying event.

These results are compared to predictions from simple coalescence and reaction-based deuteron production models. In the former approach, the phase-space distributions of nucleons are generated with PYTHIA8 with the Monash

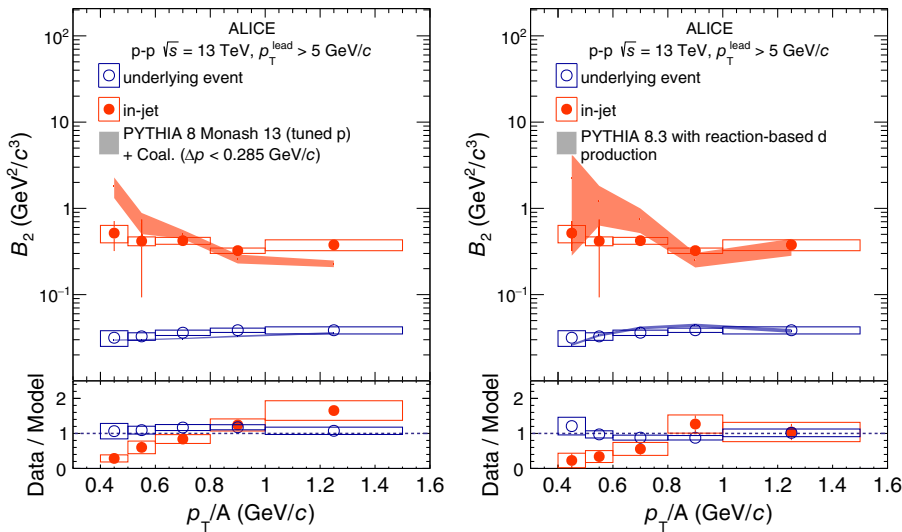


FIG. 2. Coalescence parameter in jets, B_2^{jet} , and in the underlying event, B_2^{UE} , as a function of p_T/A in comparison with the predictions from PYTHIA8 with the Monash 2013 tune with a coalescence afterburner (left panel) and the reaction-based PYTHIA8.3 model (right panel).

2013 tune [62], and their p_T spectra are reweighted to match the proton p_T spectra measured by ALICE in the three different azimuthal regions [70]. Spatial correlations are ignored and deuteron formation is assumed to happen if a proton and a neutron have a momentum difference below a given coalescence momentum $\Delta p < p_0$ in the deuteron rest frame. The best estimate of the coalescence momentum, for this model, is $p_0 = 285 \pm 1$ MeV/c, which is consistent with the value of Ref. [71]. A detailed description of these coalescence calculations can be found in the Supplemental Material [72].

In the reaction-based model [73], (anti)deuterons are generated by ordinary nuclear reactions between nucleons produced in the collision with parametrized energy-dependent cross sections tuned on available experimental data [74]. The following nuclear reactions are considered: $p + n \rightarrow \gamma + d$, $p + n \rightarrow \pi^0 + d$, $p + n \rightarrow \pi^0 + \pi^0 + d$, $p + n \rightarrow \pi^+ + \pi^- + d$, $p + p \rightarrow \pi^+ + d$, $p + p \rightarrow \pi^+ + \pi^0 + d$, $n + n \rightarrow \pi^- + d$, $n + n \rightarrow \pi^- + \pi^0 + d$. Such a model is implemented in the MC event generator PYTHIA8.3. Both simple coalescence and the reaction-based model are based on the assumption that coalescence can happen only if protons and neutrons are close in phase space. However, there are two main differences between the models. The first concerns the p_0 cutoff which is introduced as a step function in the coalescence model, while in PYTHIA8.3 the deuteron formation happens according to the differential cross section of the reactions listed above. The second difference is related to the kinematics of the process: in the coalescence model the deuteron four-momentum is given by the sum of the proton and neutron four-momenta, while in the reaction-based model, part of the initial four-momentum is carried away by the pion(s) or photon according to energy and momentum conservation rules. The uncertainties of the coalescence model are discussed in the Supplemental Material [72], while for PYTHIA8.3 only statistical uncertainties are shown.

As shown in Fig. 2, both models provide good qualitative descriptions of the data. In particular, they are capable of reproducing the observed large difference between B_2^{Jet} and B_2^{UE} . While the p_T/A dependence of B_2^{UE} is well described by both approaches within the uncertainties, the observed nearly flat trend of B_2^{Jet} is not reproduced by the models, which instead give a decreasing trend with increasing p_T/A and overestimate the B_2^{Jet} for low p_T/A .

In this Letter the first measurement of the (anti)deuteron coalescence parameters in and out of jets in p-p collisions at $\sqrt{s} = 13$ TeV is presented. The results of this Letter indicate for the first time an enhanced deuteron coalescence probability in jets compared with the underlying event. This enhancement, of a factor ~ 10 , is measured with a good precision and a significance of about 21σ . This experimental observation is a parameter-free and absolute prediction of coalescence, which decisively proves the formation of bound states by coalescence when nucleons

have a smaller average phase-space distance, as it is the case in the jet cone. This study will be extended to heavier (anti)nuclei, such as (anti) ${}^3\text{He}$, and to p-Pb collisions, with the LHC Run 3 data. Further investigations of the coalescence parameters B_A in the jet and in the underlying event, in small collision systems, which reproduce the CR interactions originating nuclei in our Galaxy, will provide additional insight into the production mechanisms and will contribute to further constrain the coalescence models. These studies will be crucial to correctly interpret any future measurement of antinuclei in satellite and balloon-borne experiments in space.

The ALICE Collaboration would like to thank all its engineers and technicians for their invaluable contributions to the construction of the experiment and the CERN accelerator teams for the outstanding performance of the LHC complex. The ALICE Collaboration gratefully acknowledges the resources and support provided by all Grid centers and the Worldwide LHC Computing Grid (WLCG) Collaboration. The ALICE Collaboration acknowledges the following funding agencies for their support in building and running the ALICE detector: A. I. Alikhanyan National Science Laboratory (Yerevan Physics Institute) Foundation (ANSL), State Committee of Science, and World Federation of Scientists (WFS), Armenia; Austrian Academy of Sciences, Austrian Science Fund (FWF): [M 2467-N36] and Nationalstiftung für Forschung, Technologie und Entwicklung, Austria; Ministry of Communications and High Technologies, National Nuclear Research Center, Azerbaijan; Conselho Nacional de Desenvolvimento Científico e Tecnológico (CNPq), Financiadora de Estudos e Projetos (Finep), Fundação de Amparo à Pesquisa do Estado de São Paulo (FAPESP), and Universidade Federal do Rio Grande do Sul (UFRGS), Brazil; Bulgarian Ministry of Education and Science, within the National Roadmap for Research Infrastructures 2020-2027 (object CERN), Bulgaria; Ministry of Education of China (MOEC), Ministry of Science & Technology of China (MSTC), and National Natural Science Foundation of China (NSFC), China; Ministry of Science and Education and Croatian Science Foundation, Croatia; Centro de Aplicaciones Tecnológicas y Desarrollo Nuclear (CEADEN), Cubaenergía, Cuba; Ministry of Education, Youth and Sports of the Czech Republic, Czech Republic; The Danish Council for Independent Research | Natural Sciences, the VILLUM FONDEN, and Danish National Research Foundation (DNRF), Denmark; Helsinki Institute of Physics (HIP), Finland; Commissariat à l'Energie Atomique (CEA) and Institut National de Physique Nucléaire et de Physique des Particules (IN2P3) and Centre National de la Recherche Scientifique (CNRS), France; Bundesministerium für Bildung und Forschung (BMBF) and GSI Helmholtzzentrum für Schwerionenforschung GmbH,

Germany; General Secretariat for Research and Technology, Ministry of Education, Research and Religions, Greece; National Research, Development and Innovation Office, Hungary; Department of Atomic Energy Government of India (DAE), Department of Science and Technology, Government of India (DST), University Grants Commission, Government of India (UGC), and Council of Scientific and Industrial Research (CSIR), India; National Research and Innovation Agency—BRIN, Indonesia; Istituto Nazionale di Fisica Nucleare (INFN), Italy; Japanese Ministry of Education, Culture, Sports, Science and Technology (MEXT) and Japan Society for the Promotion of Science (JSPS) KAKENHI, Japan; Consejo Nacional de Ciencia (CONACYT) y Tecnología, through Fondo de Cooperación Internacional en Ciencia y Tecnología (FONCICYT) and Dirección General de Asuntos del Personal Académico (DGAPA), Mexico; Nederlandse Organisatie voor Wetenschappelijk Onderzoek (NWO), Netherlands; The Research Council of Norway, Norway; Commission on Science and Technology for Sustainable Development in the South (COMSATS), Pakistan; Pontificia Universidad Católica del Perú, Peru; Ministry of Education and Science, National Science Centre, and WUT ID-UB, Poland; Korea Institute of Science and Technology Information and National Research Foundation of Korea (NRF), Republic of Korea; Ministry of Education and Scientific Research, Institute of Atomic Physics, Ministry of Research and Innovation and Institute of Atomic Physics and University Politehnica of Bucharest, Romania; Ministry of Education, Science, Research and Sport of the Slovak Republic, Slovakia; National Research Foundation of South Africa, South Africa; Swedish Research Council (VR) and Knut & Alice Wallenberg Foundation (KAW), Sweden; European Organization for Nuclear Research, Switzerland; Suranaree University of Technology (SUT), National Science and Technology Development Agency (NSTDA), Thailand Science Research and Innovation (TSRI), and National Science, Research and Innovation Fund (NSRF), Thailand; Turkish Energy, Nuclear and Mineral Research Agency (TENMAK), Turkey; National Academy of Sciences of Ukraine, Ukraine; Science and Technology Facilities Council (STFC), United Kingdom; National Science Foundation of the United States of America (NSF) and United States Department of Energy, Office of Nuclear Physics (DOE NP), United States of America. In addition, individual groups or members have received support from Marie Skłodowska Curie, European Research Council, Strong 2020—Horizon 2020 (Grants No. 950692, No. 824093, No. 896850), European Union; Academy of Finland (Center of Excellence in Quark Matter) (Grants No. 346327, No. 346328), Finland; Programa de Apoyos para la Superación del Personal Académico, UNAM, Mexico.

- [1] M. J. Bennett *et al.* (E878 Collaboration), Light nuclei production in relativistic Au + nucleus collisions, *Phys. Rev. C* **58**, 1155 (1998).
- [2] L. Ahle *et al.* (E802 Collaboration), Proton and deuteron production in Au + Au reactions at 11.6 A-GeV/c, *Phys. Rev. C* **60**, 064901 (1999).
- [3] T. A. Armstrong *et al.* (E864 Collaboration), Measurements of light nuclei production in 11.5 A-GeV/c Au + Pb heavy ion collisions, *Phys. Rev. C* **61**, 064908 (2000).
- [4] T. A. Armstrong *et al.* (E864 Collaboration), Anti-Deuteron Yield at the AGS and Coalescence Implications, *Phys. Rev. Lett.* **85**, 2685 (2000).
- [5] G. Ambrosini *et al.* (NA52 (NEWMASS) Collaboration), Baryon and anti-baryon production in lead-lead collisions at 158 A GeV/c, *Phys. Lett. B* **417**, 202 (1998).
- [6] C. Adler *et al.* (STAR Collaboration), Antideuteron and Anti-³He Production in $\sqrt{s_{NN}} = 130$ GeV Au + Au Collisions, *Phys. Rev. Lett.* **87**, 262301 (2001); **87**, 279902(E) (2001).
- [7] S. S. Adler *et al.* (PHENIX Collaboration), Deuteron and Antideuteron Production in Au + Au Collisions at 200 GeV, *Phys. Rev. Lett.* **94**, 122302 (2005).
- [8] I. Arsene *et al.* (BRAHMS Collaboration), Rapidity dependence of deuteron production in Au + Au collisions at $\sqrt{s_{NN}} = 200$ GeV, *Phys. Rev. C* **83**, 044906 (2011).
- [9] H. Agakishiev *et al.* (STAR Collaboration), Observation of the antimatter helium-4 nucleus, *Nature (London)* **473**, 353 (2011); **475**, 412(E) (2011).
- [10] L. Adamczyk *et al.* (STAR Collaboration), Measurement of elliptic flow of light nuclei at $\sqrt{s_{NN}} = 200, 62.4, 39, 27, 19.6, 11.5$, and 7.7 GeV at the BNL Relativistic Heavy Ion Collider, *Phys. Rev. C* **94**, 034908 (2016).
- [11] J. Adam *et al.* (STAR Collaboration), Beam energy dependence of (anti-)deuteron production in Au + Au collisions at the BNL Relativistic Heavy Ion Collider, *Phys. Rev. C* **99**, 064905 (2019).
- [12] J. Adam *et al.* (ALICE Collaboration), Precision measurement of the mass difference between light nuclei and anti-nuclei, *Nat. Phys.* **11**, 811 (2015).
- [13] J. Adam *et al.* (ALICE Collaboration), Production of light nuclei and anti-nuclei in pp and Pb–Pb collisions at energies available at the CERN Large Hadron Collider, *Phys. Rev. C* **93**, 024917 (2016).
- [14] S. Acharya *et al.* (ALICE Collaboration), Multiplicity dependence of (anti-)deuteron production in pp collisions at $\sqrt{s} = 7$ TeV, *Phys. Lett. B* **794**, 50 (2019).
- [15] S. Acharya *et al.* (ALICE Collaboration), Measurement of deuteron spectra and elliptic flow in Pb–Pb collisions at $\sqrt{s_{NN}} = 2.76$ TeV at the LHC, *Eur. Phys. J. C* **77**, 658 (2017).
- [16] S. Acharya *et al.* (ALICE Collaboration), Production of deuterons, tritons, ³He nuclei and their antinuclei in pp collisions at $\sqrt{s} = 0.9, 2.76$ and 7 TeV, *Phys. Rev. C* **97**, 024615 (2018).
- [17] S. Acharya *et al.* (ALICE Collaboration), Production of ⁴He and ⁴ \bar{He} in Pb–Pb collisions at $\sqrt{s_{NN}} = 2.76$ TeV at the LHC, *Nucl. Phys.* **A971**, 1 (2018).
- [18] S. Acharya *et al.* (ALICE Collaboration), Multiplicity dependence of light (anti-)nuclei production in p–Pb collisions at $\sqrt{s_{NN}} = 5.02$ TeV, *Phys. Lett. B* **800**, 135043 (2020).

- [19] S. Acharya *et al.* (ALICE Collaboration), Production of (anti-) ^3He and (anti-) ^3H in p–Pb collisions at $\sqrt{s_{\text{NN}}} = 5.02$ TeV, *Phys. Rev. C* **101**, 044906 (2020).
- [20] S. Acharya *et al.* (ALICE Collaboration), (Anti-)deuteron production in pp collisions at $\sqrt{s} = 13$ TeV, *Eur. Phys. J. C* **80**, 889 (2020).
- [21] S. Acharya *et al.* (ALICE Collaboration), Production of light (anti)nuclei in pp collisions at $\sqrt{s} = 13$ TeV, *J. High Energy Phys.* **01** (2022) 106.
- [22] S. Acharya *et al.* (ALICE Collaboration), Jet-associated deuteron production in pp collisions at $\sqrt{s} = 13$ TeV, *Phys. Lett. B* **819**, 136440 (2021).
- [23] S. Acharya *et al.* (ALICE Collaboration), Production of light (anti)nuclei in pp collisions at $\sqrt{s} = 5.02$ TeV, *Eur. Phys. J. C* **82**, 289 (2022).
- [24] S. Acharya *et al.* (ALICE Collaboration), Hypertriton Production in p–Pb Collisions at $\sqrt{s_{\text{NN}}} = 5.02$ TeV, *Phys. Rev. Lett.* **128**, 252003 (2022).
- [25] S. Acharya *et al.* (ALICE Collaboration), Measurement of deuteron spectra and elliptic flow in Pb–Pb collisions at $\sqrt{s_{\text{NN}}} = 2.76$ TeV at the LHC, *Eur. Phys. J. C* **77**, 658 (2017).
- [26] S. Acharya *et al.* (ALICE Collaboration), Elliptic and triangular flow of (anti)deuterons in Pb–Pb collisions at $\sqrt{s_{\text{NN}}} = 5.02$ TeV, *Phys. Rev. C* **102**, 055203 (2020).
- [27] S. Acharya *et al.* (ALICE Collaboration), Measurement of the (anti-) ^3He elliptic flow in Pb–Pb collisions at $\sqrt{s_{\text{NN}}} = 5.02$ TeV, *Phys. Lett. B* **805**, 135414 (2020).
- [28] S. T. Butler and C. A. Pearson, Deuterons from high-energy proton bombardment of matter, *Phys. Rev.* **129**, 836 (1963).
- [29] J. I. Kapusta, Mechanisms for deuteron production in relativistic nuclear collisions, *Phys. Rev. C* **21**, 1301 (1980).
- [30] R. Scheibl and U. W. Heinz, Coalescence and flow in ultrarelativistic heavy ion collisions, *Phys. Rev. C* **59**, 1585 (1999).
- [31] W. Zhao, L. Zhu, H. Zheng, C. M. Ko, and H. Song, Spectra and flow of light nuclei in relativistic heavy ion collisions at energies available at the BNL Relativistic Heavy Ion Collider and at the CERN Large Hadron Collider, *Phys. Rev. C* **98**, 054905 (2018).
- [32] K. Blum and M. Takimoto, Nuclear coalescence from correlation functions, *Phys. Rev. C* **99**, 044913 (2019).
- [33] K.-J. Sun, C. M. Ko, and B. Dönigus, Suppression of light nuclei production in collisions of small systems at the Large Hadron Collider, *Phys. Lett. B* **792**, 132 (2019).
- [34] M. Kachelrieß, S. Ostapchenko, and J. Tjemsland, Alternative coalescence model for deuteron, tritium, helium-3 and their antinuclei, *Eur. Phys. J. A* **56**, 4 (2020).
- [35] D. Oliinychenko, L.-G. Pang, H. Elfner, and V. Koch, Microscopic study of deuteron production in Pb–Pb collisions at $\sqrt{s_{\text{NN}}} = 2.76$ TeV via hydrodynamics and a hadronic afterburner, *Phys. Rev. C* **99**, 044907 (2019).
- [36] J. Cleymans, S. Kabana, I. Kraus, H. Oeschler, K. Redlich, and N. Sharma, Antimatter production in proton-proton and heavy-ion collisions at ultrarelativistic energies, *Phys. Rev. C* **84**, 054916 (2011).
- [37] A. Andronic, P. Braun-Munzinger, J. Stachel, and H. Stöcker, Production of light nuclei, hypernuclei and their antiparticles in relativistic nuclear collisions, *Phys. Lett. B* **697**, 203 (2011).
- [38] F. Becattini, M. Bleicher, E. Grossi, J. Steinheimer, and R. Stock, Centrality dependence of hadronization and chemical freeze-out conditions in heavy ion collisions at $\sqrt{s_{\text{NN}}} = 2.76$ TeV, *Phys. Rev. C* **90**, 054907 (2014).
- [39] V. Vovchenko and H. Stöcker, Examination of the sensitivity of the thermal fits to heavy-ion hadron yield data to the modeling of the eigenvolume interactions, *Phys. Rev. C* **95**, 044904 (2017).
- [40] A. Andronic, P. Braun-Munzinger, K. Redlich, and J. Stachel, Decoding the phase structure of QCD via particle production at high energy, *Nature (London)* **561**, 321 (2018).
- [41] N. Sharma, J. Cleymans, B. Hippolyte, and M. Paradza, A comparison of p-p, p–Pb, Pb–Pb collisions in the thermal model: Multiplicity dependence of thermal parameters, *Phys. Rev. C* **99**, 044914 (2019).
- [42] V. Vovchenko, B. Dönigus, and H. Stoecker, Canonical statistical model analysis of p-p, p–Pb, and Pb–Pb collisions at energies available at the CERN Large Hadron Collider, *Phys. Rev. C* **100**, 054906 (2019).
- [43] V. Vovchenko, B. Dönigus, and H. Stoecker, Multiplicity dependence of light nuclei production at LHC energies in the canonical statistical model, *Phys. Lett. B* **785**, 171 (2018).
- [44] A. Kounine, The alpha magnetic spectrometer on the international space station, *Int. J. Mod. Phys. E* **21**, 1230005 (2012).
- [45] C. J. Hailey, An indirect search for dark matter using anti-deuterons: The GAPS experiment, *New J. Phys.* **11**, 105022 (2009).
- [46] F. Donato, N. Fornengo, and D. Maurin, Antideuteron fluxes from dark matter annihilation in diffusion models, *Phys. Rev. D* **78**, 043506 (2008).
- [47] M. Korsmeier, F. Donato, and N. Fornengo, Prospects to verify a possible dark matter hint in cosmic antiprotons with antideuterons and antihelium, *Phys. Rev. D* **97**, 103011 (2018).
- [48] M. Aguilar *et al.* (AMS Collaboration), Antiproton Flux, Antiproton-to-Proton Flux Ratio, and Properties of Elementary Particle Fluxes in Primary Cosmic Rays Measured with the Alpha Magnetic Spectrometer on the International Space Station, *Phys. Rev. Lett.* **117**, 091103 (2016).
- [49] S. Acharya *et al.* (ALICE Collaboration), Measurement of the Low-Energy Antideuteron Inelastic Cross Section, *Phys. Rev. Lett.* **125**, 162001 (2020).
- [50] R. D. Field and R. P. Feynman, A parametrization of the properties of quark jets, *Nucl. Phys.* **B136**, 1 (1978).
- [51] B. Andersson, G. Gustafson, G. Ingelman, and T. Sjostrand, Parton fragmentation and string dynamics, *Phys. Rep.* **97**, 31 (1983).
- [52] T. Sjostrand, S. Mrenna, and P. Z. Skands, A brief introduction to PYTHIA8.1, *Comput. Phys. Commun.* **178**, 852 (2008).
- [53] S. Acharya *et al.* (ALICE Collaboration), Supplemental Material: Afterburner for generating light (anti)-nuclei with QCD-inspired event generators in pp collisions, Report No. ALICE-PUBLIC-2017-010, 2017, <https://cds.cern.ch/record/2285500>.
- [54] S. Acharya *et al.* (ALICE Collaboration), Underlying event properties in pp collisions at $\sqrt{s} = 13$ TeV, *J. High Energy Phys.* **04** (2020) 192.
- [55] ALICE Collaboration, Underlying-event properties in pp and p–Pb collisions at $\sqrt{s_{\text{NN}}} = 5.02$ TeV, [arXiv:2204.10389](https://arxiv.org/abs/2204.10389).

- [56] K. Aamodt *et al.* (ALICE Collaboration), The ALICE experiment at the CERN LHC, *J. Instrum.* **3**, S08002 (2008).
- [57] B. Abelev *et al.* (ALICE Collaboration), Performance of the ALICE experiment at the CERN LHC, *Int. J. Mod. Phys. A* **29**, 1430044 (2014).
- [58] J. Alme *et al.*, The ALICE TPC, a large 3-dimensional tracking device with fast readout for ultra-high multiplicity events, *Nucl. Instrum. Methods Phys. Res., Sect. A* **622**, 316 (2010).
- [59] A. Akindinov *et al.* (ALICE Collaboration), Performance of the ALICE time-of-flight detector at the LHC, *Eur. Phys. J. Plus* **128**, 44 (2013).
- [60] J. Adam *et al.* (ALICE Collaboration), Determination of the event collision time with the ALICE detector at the LHC, *Eur. Phys. J. Plus* **132**, 99 (2017).
- [61] P. Cortese *et al.* (ALICE Collaboration), ALICE technical design report on forward detectors: FMD, T0 and V0, Report No. CERN-LHCC-2004-025, 2004, <http://cds.cern.ch/record/781854>.
- [62] P. Skands, S. Carrazza, and J. Rojo, Tuning PYTHIA8.1: The Monash 2013 tune, *Eur. Phys. J. C* **74**, 3024 (2014).
- [63] S. Agostinelli *et al.* (GEANT4 Collaboration), GEANT4—a simulation toolkit, *Nucl. Instrum. Methods Phys. Res., Sect. A* **506**, 250 (2003).
- [64] J. Jaros *et al.*, Nucleus-nucleus total cross sections for light nuclei at 1.55 and 2.89 GeV/c per nucleon, *Phys. Rev. C* **18**, 2273 (1978).
- [65] A. Auce, R. F. Carlson, A. J. Cox, A. Ingemarsson, R. Johansson, P. U. Renberg, O. Sundberg, and G. Tibell, Reaction cross sections for 38, 65, and 97 MeV deuterons on targets from ${}^9\text{Be}$ to ${}^{208}\text{Pb}$, *Phys. Rev. C* **53**, 2919 (1996).
- [66] S. P. Denisov, S. V. Donskov, Yu. P. Gorin, V. A. Kachanov, V. M. Kutjin, A. I. Petrukhin, Yu. D. Prokoshkin, E. A. Razuvaev, R. S. Shuvalov, and D. A. Stojanova, Measurements of anti-deuteron absorption and stripping cross sections at the momentum 13.3 GeV/c, *Nucl. Phys.* **B31**, 253 (1971).
- [67] F. G. Binon *et al.*, Absorption cross-sections of 25 GeV/c antideuterons in Li, C, Al, Cu and Pb, *Phys. Lett.* **31B**, 230 (1970).
- [68] C. Tsallis, Possible generalization of Boltzmann-Gibbs statistics, *J. Stat. Phys.* **52**, 479 (1988).
- [69] S. S. Adler *et al.* (PHENIX Collaboration), Dense-Medium Modifications to Jet-Induced Hadron Pair Distributions in Au + Au Collisions at $\sqrt{s_{\text{NN}}} = 200$ GeV, *Phys. Rev. Lett.* **97**, 052301 (2006).
- [70] ALICE Collaboration, Production of pions, kaons and protons as a function of the transverse event activity in pp collisions at $\sqrt{s} = 13$ TeV, [arXiv:2301.10120](https://arxiv.org/abs/2301.10120).
- [71] S. Sombun, K. Tomuang, A. Limphirat, P. Hillmann, C. Herold, J. Steinheimer, Y. Yan, and M. Bleicher, Deuteron production from phase-space coalescence in the UrQMD approach, *Phys. Rev. C* **99**, 014901 (2019).
- [72] See Supplemental Material at <http://link.aps.org/supplemental/10.1103/PhysRevLett.131.042301> for additional figures.
- [73] C. Bierlich *et al.*, A comprehensive guide to the physics and usage of PYTHIA8.3, *SciPost Phys. Codebases*, [10.21468/SciPostPhysCodeb.8](https://doi.org/10.21468/SciPostPhysCodeb.8) (2022).
- [74] L. A. Dal and A. R. Raklev, Alternative formation model for antideuterons from dark matter, *Phys. Rev. D* **91**, 123536 (2015); **92**, 069903(E) (2015); **92**, 089901(E) (2015).

S. Acharya¹²⁵ D. Adamová⁸⁶ A. Adler⁶⁹ G. Aglieri Rinella³² M. Agnello²⁹ N. Agrawal⁵⁰ Z. Ahammed¹³²
 S. Ahmad¹⁵ S. U. Ahn⁷⁰ I. Ahuja³⁷ A. Akindinov¹⁴⁰ M. Al-Turany⁹⁷ D. Aleksandrov¹⁴⁰ B. Alessandro⁵⁵
 H. M. Alfanda⁶ R. Alfaro Molina⁶⁶ B. Ali¹⁵ A. Alici²⁵ N. Alizadehvandchali¹¹⁴ A. Alkin³² J. Alme²⁰
 G. Alocco⁵¹ T. Alt⁶³ I. Altsybeev¹⁴⁰ M. N. Anaam⁶ C. Andrei⁴⁵ A. Andronic¹³⁵ V. Anguelov⁹⁴
 F. Antinori⁵³ P. Antonioli⁵⁰ N. Apadula⁷⁴ L. Aphecetche¹⁰³ H. Appelshäuser⁶³ C. Arata⁷³ S. Arcelli²⁵
 M. Aresti⁵¹ R. Arnaldi⁵⁵ J. G. M. C. A. Arneiro¹¹⁰ I. C. Arsene¹⁹ M. Arslandok¹³⁷ A. Augustinus³²
 R. Averbbeck⁹⁷ M. D. Azmi¹⁵ A. Badalà⁵² J. Bae¹⁰⁴ Y. W. Baek⁴⁰ X. Bai¹¹⁸ R. Bailhache⁶³ Y. Bailung⁴⁷
 A. Balbino²⁹ A. Baldisseri¹²⁸ B. Balis² D. Banerjee⁴ Z. Banoo⁹¹ R. Barbera²⁶ F. Barile³¹ L. Barioglio⁹⁵
 M. Barlou⁷⁸ G. G. Barnaföldi¹³⁶ L. S. Barnby⁸⁵ V. Barret¹²⁵ L. Barreto¹¹⁰ C. Bartels¹¹⁷ K. Barth³²
 E. Bartsch⁶³ N. Bastid¹²⁵ S. Basu⁷⁵ G. Batigne¹⁰³ D. Battistini⁹⁵ B. Batyunya¹⁴¹ D. Bauri,⁴⁶
 J. L. Bazo Alba¹⁰¹ I. G. Bearden⁸³ C. Beattie¹³⁷ P. Becht⁹⁷ D. Behera⁴⁷ I. Belikov¹²⁷
 A. D. C. Bell Hechavarria¹³⁵ F. Bellini²⁵ R. Bellwied¹¹⁴ S. Belokurova¹⁴⁰ V. Belyaev¹⁴⁰ G. Bencedi¹³⁶
 S. Beole²⁴ A. Bercuci⁴⁵ Y. Berdnikov¹⁴⁰ A. Berdnikova⁹⁴ L. Bergmann⁹⁴ M. G. Besoiu⁶² L. Betev³²
 P. P. Bhaduri¹³² A. Bhasin⁹¹ M. A. Bhat⁴ B. Bhattacharjee⁴¹ L. Bianchi²⁴ N. Bianchi⁴⁸ J. Bielčík³⁵
 J. Bielčíková⁸⁶ J. Biernat¹⁰⁷ A. P. Bigot¹²⁷ A. Bilandžić⁹⁵ G. Biro¹³⁶ S. Biswas⁴ N. Bize¹⁰³ J. T. Blair¹⁰⁸
 D. Blau¹⁴⁰ M. B. Blidaru⁹⁷ N. Bluhme³⁸ C. Blume⁶³ G. Boca^{21,54} F. Bock⁸⁷ T. Bodova²⁰ A. Bogdanov,¹⁴⁰
 S. Boi²² J. Bok⁵⁷ L. Boldizsár¹³⁶ A. Bolozdynya¹⁴⁰ M. Bombara³⁷ P. M. Bond³² G. Bonomi^{131,54}
 H. Borel¹²⁸ A. Borissov¹⁴⁰ A. G. Borquez Carcamo⁹⁴ H. Bossi¹³⁷ E. Botta²⁴ Y. E. M. Bouziani⁶³
 L. Bratrud⁶³ P. Braun-Munzinger⁹⁷ M. Bregant¹¹⁰ M. Broz³⁵ G. E. Bruno^{96,31} M. D. Buckland²³
 D. Budnikov¹⁴⁰ H. Buesching⁶³ S. Bufalino²⁹ O. Bugnon,¹⁰³ P. Buhler¹⁰² Z. Buthelezi^{67,121} S. A. Bysiak,¹⁰⁷

- M. Cai⁶ H. Caines¹³⁷ A. Caliva⁹⁷ E. Calvo Villar¹⁰¹ J. M. M. Camacho¹⁰⁹ P. Camerini²³ F. D. M. Canedo¹¹⁰
 M. Carabas¹²⁴ A. A. Carballo³² F. Carnesecchi³² R. Caron¹²⁶ L. A. D. Carvalho¹¹⁰ J. Castillo Castellanos¹²⁸
 F. Catalano^{24,29} C. Ceballos Sanchez¹⁴¹ I. Chakaberia⁷⁴ P. Chakraborty⁴⁶ S. Chandra¹³² S. Chapelend³²
 M. Chartier¹¹⁷ S. Chattopadhyay¹³² S. Chattopadhyay⁹⁹ T. G. Chavez⁴⁴ T. Cheng^{97,6} C. Cheshkov¹²⁶
 B. Cheynis¹²⁶ V. Chibante Barroso³² D. D. Chinellato¹¹¹ E. S. Chizzali^{95,b} J. Cho⁵⁷ S. Cho⁵⁷ P. Chochula³²
 P. Christakoglou⁸⁴ C. H. Christensen⁸³ P. Christiansen⁷⁵ T. Chujo¹²³ M. Ciacco²⁹ C. Cicalo⁵¹ F. Cindolo⁵⁰
 M. R. Ciupek⁹⁷ G. Clai,^{50,c} F. Colamaria⁴⁹ J. S. Colburn,¹⁰⁰ D. Colella^{96,31} M. Colocci³² M. Concas^D,
 G. Conesa Balbastre⁷³ Z. Conesa del Valle⁷² G. Contin²³ J. G. Contreras³⁵ M. L. Coquet¹²⁸ T. M. Cormier,^{87,a}
 P. Cortese^{130,55} M. R. Cosentino¹¹² F. Costa³² S. Costanza^{21,54} C. Cot⁷² J. Crkovská⁹⁴ P. Crochet¹²⁵
 R. Cruz-Torres⁷⁴ E. Cuautle,⁶⁴ P. Cui⁶ A. Dainese⁵³ M. C. Danisch⁹⁴ A. Danu⁶² P. Das⁸⁰ P. Das⁴ S. Das^b
 A. R. Dash¹³⁵ S. Dash⁴⁶ R. M. H. David,⁴⁴ A. De Caro²⁸ G. de Cataldo⁴⁹ J. de Cuveland,³⁸ A. De Falco²²
 D. De Gruttola²⁸ N. De Marco⁵⁵ C. De Martin²³ S. De Pasquale²⁸ S. Deb⁴⁷ R. J. Debski² K. R. Deja,¹³³
 R. Del Grande⁹⁵ L. Dello Stritto²⁸ W. Deng⁶ P. Dhankher¹⁸ D. Di Bari³¹ A. Di Mauro³² R. A. Diaz^b,^{7,141}
 T. Dietel¹¹³ Y. Ding^{126,6} R. Divià³² D. U. Dixit¹⁸ Ø. Djuvland²⁰ U. Dmitrieva¹⁴⁰ A. Dobrin⁶² B. Dönigus⁶³
 J. M. Dubinski¹³³ A. Dubla⁹⁷ S. Dudi⁹⁰ P. Dupieux¹²⁵ M. Durkac,¹⁰⁶ N. Dzalaiova,¹² T. M. Eder¹³⁵
 R. J. Ehlers⁸⁷ V. N. Eikeland²⁰ F. Eisenhut⁶³ D. Elia⁴⁹ B. Erazmus¹⁰³ F. Ercolelli²⁵ F. Erhardt⁸⁹
 M. R. Ersdal²⁰ B. Espagnon⁷² G. Eulisse³² D. Evans¹⁰⁰ S. Evdokimov¹⁴⁰ L. Fabbietti⁹⁵ M. Faggin²⁷
 J. Faivre⁷³ F. Fan⁶ W. Fan⁷⁴ A. Fantoni⁴⁸ M. Fasel⁸⁷ P. Fecchio,²⁹ A. Feliciello⁵⁵ G. Feofilov¹⁴⁰
 A. Fernández Téllez⁴⁴ L. Ferrandi¹¹⁰ M. B. Ferrer^D,³² A. Ferrero¹²⁸ C. Ferrero⁵⁵ A. Ferretti²⁴
 V. J. G. Feuillard⁹⁴ V. Filova³⁵ D. Finogeev¹⁴⁰ F. M. Fionda⁵¹ F. Flor¹¹⁴ A. N. Flores¹⁰⁸ S. Foertsch⁶⁷
 I. Fokin⁹⁴ S. Fokin¹⁴⁰ E. Fragiocomo⁵⁶ E. Frajna¹³⁶ U. Fuchs³² N. Funicello²⁸ C. Furget⁷³ A. Furs^D,¹⁴⁰
 T. Fusayasu⁹⁸ J. J. Gaardhøje⁸³ M. Gagliardi²⁴ A. M. Gago¹⁰¹ C. D. Galvan¹⁰⁹ D. R. Gangadharan^D,¹¹⁴
 P. Ganoti⁷⁸ C. Garabatos⁹⁷ J. R. A. Garcia⁴⁴ E. Garcia-Solis⁹ K. Garg¹⁰³ C. Gargiulo³² K. Garner,¹³⁵
 P. Gasik⁹⁷ A. Gautam¹¹⁶ M. B. Gay Ducati⁶⁵ M. Germain¹⁰³ A. Ghimouz,¹²³ C. Ghosh,¹³² M. Giacalone^D,^{50,25}
 P. Giubellino^{97,55} P. Giubilato²⁷ A. M. C. Glaenzer¹²⁸ P. Glässel⁹⁴ E. Glimos¹²⁰ D. J. Q. Goh,⁷⁶ V. Gonzalez^D,¹³⁴
 L. H. González-Trueba⁶⁶ M. Gorgon² S. Gotovac,³³ V. Grabski⁶⁶ L. K. Graczykowski¹³³ E. Grecka⁸⁶
 A. Grelli⁵⁸ C. Grigoras³² V. Grigoriev¹⁴⁰ S. Grigoryan^{141,1} F. Grossa³² J. F. Grosse-Oetringhaus^D,³²
 R. Grossos⁹⁷ D. Grund³⁵ G. G. Guardiano¹¹¹ R. Guernane⁷³ M. Guilbaud¹⁰³ K. Gulbrandsen⁸³ T. Gundem⁶³
 T. Gunji¹²² W. Guo⁶ A. Gupta⁹¹ R. Gupta⁹¹ S. P. Guzman⁴⁴ L. Gyulai¹³⁶ M. K. Habib,⁹⁷ C. Hadjidakis^D,⁷²
 F. U. Haider⁹¹ H. Hamagaki⁷⁶ A. Hamdi⁷⁴ M. Hamid,⁶ Y. Han¹³⁸ R. Hannigan¹⁰⁸ M. R. Haque^D,¹³³
 J. W. Harris¹³⁷ A. Harton⁹ H. Hassan⁸⁷ D. Hatzifotiadou⁵⁰ P. Hauer⁴² L. B. Havener¹³⁷ S. T. Heckel^D,⁹⁵
 E. Hellbär⁹⁷ H. Helstrup³⁴ M. Hemmer⁶³ T. Herman³⁵ G. Herrera Corral⁸ F. Herrmann,¹³⁵ S. Herrmann^D,¹²⁶
 K. F. Hetland³⁴ B. Heybeck⁶³ H. Hillemanns³² C. Hills¹¹⁷ B. Hippolyte¹²⁷ F. W. Hoffmann⁶⁹ B. Hofman⁵⁸
 B. Hohlweger⁸⁴ G. H. Hong¹³⁸ M. Horst⁹⁵ A. Horzyk² R. Hosokawa,¹⁴ Y. Hou⁶ P. Hristov³² C. Hughes^D,¹²⁰
 P. Huhn,⁶³ L. M. Huhta¹¹⁵ C. V. Hulse⁷² T. J. Humanic^D,⁸⁸ A. Hutson¹¹⁴ D. Hutter³⁸ J. P. Iddon¹¹⁷ R. Ilkaev,¹⁴⁰
 H. Ilyas¹³ M. Inaba¹²³ G. M. Innocenti³² M. Ippolitov¹⁴⁰ A. Isakov⁸⁶ T. Isidori¹¹⁶ M. S. Islam⁹⁹
 M. Ivanov,¹² M. Ivanov⁹⁷ V. Ivanov¹⁴⁰ M. Jablonski² B. Jacak⁷⁴ N. Jacazio³² P. M. Jacobs⁷⁴ S. Jadlovska,¹⁰⁶
 J. Jadlovsky,¹⁰⁶ S. Jaelani⁸² L. Jaffe,³⁸ C. Jahnke¹¹¹ M. J. Jakubowska¹³³ M. A. Janik¹³³ T. Janson,⁶⁹ M. Jercic,⁸⁹
 S. Jia¹⁰ A. A. P. Jimenez⁶⁴ F. Jonas⁸⁷ J. M. Jowett^{32,97} J. Jung⁶³ M. Jung⁶³ A. Junique³² A. Jusko¹⁰⁰
 M. J. Kabus^{32,133} J. Kaewjai,¹⁰⁵ P. Kalinak⁵⁹ A. S. Kalteyer⁹⁷ A. Kalweit³² V. Kaplin¹⁴⁰ A. Karasu Uysal,⁷¹
 D. Karatovic⁸⁹ O. Karavichev¹⁴⁰ T. Karavicheva¹⁴⁰ P. Karczmarczyk¹³³ E. Karpechev^D,¹⁴⁰ U. Kebeschull⁶⁹
 R. Keidel¹³⁹ D. L. D. Keijdener,⁵⁸ M. Keil³² B. Ketzer⁴² A. M. Khan⁶ S. Khan¹⁵ A. Khanzadeev^D,¹⁴⁰
 Y. Kharlov¹⁴⁰ A. Khatun^{116,15} A. Khuntia¹⁰⁷ M. B. Kidson,¹¹³ B. Kileng³⁴ B. Kim¹⁶ C. Kim¹⁶ D. J. Kim^D,¹¹⁵
 E. J. Kim⁶⁸ J. Kim¹³⁸ J. S. Kim⁴⁰ J. Kim⁶⁸ M. Kim^{18,94} S. Kim¹⁷ T. Kim¹³⁸ K. Kimura⁹² S. Kirsch⁶³
 I. Kisel³⁸ S. Kiselev¹⁴⁰ A. Kisiel¹³³ J. P. Kitowski² J. L. Klay⁵ J. Klein³² S. Klein⁷⁴ C. Klein-Bösing^D,¹³⁵
 M. Kleiner⁶³ T. Klemenz⁹⁵ A. Kluge³² A. G. Knospe¹¹⁴ C. Kobdaj¹⁰⁵ T. Kollegger,⁹⁷ A. Kondratyev^D,¹⁴¹
 N. Kondratyeva¹⁴⁰ E. Kondratyuk¹⁴⁰ J. Konig⁶³ S. A. Konigstorfer⁹⁵ P. J. Konopka³² G. Kornakov^D,¹³³
 S. D. Koryciak² A. Kotliarov⁸⁶ V. Kovalenko¹⁴⁰ M. Kowalski¹⁰⁷ V. Kozhuharov³⁶ I. Králik⁵⁹
 A. Kravčáková³⁷ L. Kreis,⁹⁷ M. Krivda^{100,59} F. Krizek⁸⁶ K. Krizkova Gajdosova³⁵ M. Kroesen⁹⁴ M. Krüger^D,⁶³

- D. M. Krupova¹,³⁵ E. Kryshen¹,¹⁴⁰ V. Kučera¹,³² C. Kuhn¹,¹²⁷ P. G. Kuijer¹,⁸⁴ T. Kumaoka,¹²³ D. Kumar,¹³²
 L. Kumar,⁹⁰ N. Kumar,⁹⁰ S. Kumar¹,³¹ S. Kundu¹,³² P. Kurashvili¹,⁷⁹ A. Kurepin¹,¹⁴⁰ A. B. Kurepin¹,¹⁴⁰
 A. Kuryakin¹,¹⁴⁰ S. Kushpil¹,⁸⁶ J. Kvapil¹,¹⁰⁰ M. J. Kweon¹,⁵⁷ J. Y. Kwon¹,⁵⁷ Y. Kwon¹,¹³⁸ S. L. La Pointe¹,³⁸
 P. La Rocca¹,²⁶ Y. S. Lai,⁷⁴ A. Lakrathok,¹⁰⁵ M. Lamanna¹,³² R. Langoy¹,¹¹⁹ P. Larionov¹,³² E. Laudi¹,³²
 L. Lautner¹,^{32,95} R. Lavicka¹,¹⁰² T. Lazareva¹,¹⁴⁰ R. Lea¹,^{131,54} H. Lee¹,¹⁰⁴ G. Legras¹,¹³⁵ J. Lehrbach¹,³⁸
 R. C. Lemmon¹,⁸⁵ I. León Monzón¹,¹⁰⁹ M. M. Lesch¹,⁹⁵ E. D. Lesser¹,¹⁸ M. Lettrich,⁹⁵ P. Lévai¹,¹³⁶ X. Li,¹⁰ X. L. Li,⁶
 J. Lien¹,¹¹⁹ R. Lietava¹,¹⁰⁰ I. Likmeta¹,¹¹⁴ B. Lim¹,^{24,16} S. H. Lim¹,¹⁶ V. Lindenstruth¹,³⁸ A. Lindner,⁴⁵
 C. Lippmann¹,⁹⁷ A. Liu¹,¹⁸ D. H. Liu¹,⁶ J. Liu¹,¹¹⁷ I. M. Lofnes¹,²⁰ C. Loizides¹,⁸⁷ S. Lokos¹,¹⁰⁷ J. Lomker¹,⁵⁸
 P. Loncar¹,³³ J. A. Lopez¹,⁹⁴ X. Lopez¹,¹²⁵ E. López Torres¹,⁷ P. Lu¹,^{97,118} J. R. Luhder¹,¹³⁵ M. Lunardon¹,²⁷
 G. Luparello¹,⁵⁶ Y. G. Ma¹,³⁹ A. Maevskaia,¹⁴⁰ M. Mager¹,³² T. Mahmoud,⁴² A. Maire¹,¹²⁷ M. V. Makarieva¹,³⁶
 M. Malaei¹,¹⁴⁰ G. Malfattore¹,²⁵ N. M. Malik¹,⁹¹ Q. W. Malik,¹⁹ S. K. Malik¹,⁹¹ L. Malinina¹,^{141,g} D. Mal'Kevich¹,¹⁴⁰
 D. Mallick¹,⁸⁰ N. Mallick¹,⁴⁷ G. Mandaglio¹,^{30,52} V. Manko¹,¹⁴⁰ F. Manso¹,¹²⁵ V. Manzari¹,⁴⁹ Y. Mao¹,⁶
 G. V. Margagliotti¹,²³ A. Margotti¹,⁵⁰ A. Marín¹,⁹⁷ C. Markert¹,¹⁰⁸ P. Martinengo¹,³² J. L. Martinez,¹¹⁴
 M. I. Martínez¹,⁴⁴ G. Martínez García¹,¹⁰³ S. Masciocchi¹,⁹⁷ M. Masera¹,²⁴ A. Masoni¹,⁵¹ L. Massacrier¹,⁷²
 A. Mastroserio¹,^{129,49} O. Matonoha¹,⁷⁵ P. F. T. Matuoka,¹¹⁰ A. Matyja¹,¹⁰⁷ C. Mayer¹,¹⁰⁷ A. L. Mazuecos¹,³²
 F. Mazzaschi¹,²⁴ M. Mazzilli¹,³² J. E. Mdhluli¹,¹²¹ A. F. Mechler,⁶³ Y. Melikyan¹,^{43,140} A. Menchaca-Rocha¹,⁶⁶
 E. Meninno¹,^{102,28} A. S. Menon¹,¹¹⁴ M. Meres¹,¹² S. Mhlanga,^{113,67} Y. Miake,¹²³ L. Micheletti¹,⁵⁵ L. C. Migliorin,¹²⁶
 D. L. Mihaylov¹,⁹⁵ K. Mikhaylov¹,^{141,140} A. N. Mishra¹,¹³⁶ D. Miśkowiec¹,⁹⁷ A. Modak¹,⁴ A. P. Mohanty¹,⁵⁸
 B. Mohanty,⁸⁰ M. Mohisin Khan¹,^{15,e} M. A. Molander¹,⁴³ Z. Moravcova¹,⁸³ C. Mordasini¹,⁹⁵
 D. A. Moreira De Godoy¹,¹³⁵ I. Morozov¹,¹⁴⁰ A. Morsch¹,³² T. Mrnjavac¹,³² V. Muccifora¹,⁴⁸ S. Muhuri¹,¹³²
 J. D. Mulligan¹,⁷⁴ A. Mulliri,²² M. G. Munhoz¹,¹¹⁰ R. H. Munzer¹,⁶³ H. Murakami¹,¹²² S. Murray¹,¹¹³ L. Musa¹,³²
 J. Musinsky¹,⁵⁹ J. W. Myrcha¹,¹³³ B. Naik¹,¹²¹ A. I. Nambrath¹,¹⁸ B. K. Nandi¹,⁴⁶ R. Nania¹,⁵⁰ E. Nappi¹,⁴⁹
 A. F. Nassirpour¹,⁷⁵ A. Nath¹,⁹⁴ C. Nattrass¹,¹²⁰ M. N. Naydenov¹,³⁶ A. Neagu,¹⁹ A. Negru,¹²⁴ L. Nellen¹,⁶⁴
 S. V. Nesbo,³⁴ G. Neskovic¹,³⁸ D. Nesterov¹,¹⁴⁰ B. S. Nielsen¹,⁸³ E. G. Nielsen¹,⁸³ S. Nikolaev¹,¹⁴⁰ S. Nikulin¹,¹⁴⁰
 V. Nikulin¹,¹⁴⁰ F. Noferini¹,⁵⁰ S. Noh¹,¹¹ P. Nomokonov¹,¹⁴¹ J. Norman¹,¹¹⁷ N. Novitzky¹,¹²³ P. Nowakowski¹,¹³³
 A. Nyanin¹,¹⁴⁰ J. Nystrand¹,²⁰ M. Ogino¹,⁷⁶ A. Ohlson¹,⁷⁵ V. A. Okorokov¹,¹⁴⁰ J. Oleniacz¹,¹³³
 A. C. Oliveira Da Silva¹,¹²⁰ M. H. Oliver¹,¹³⁷ A. Onnerstad¹,¹¹⁵ C. Oppedisano¹,⁵⁵ A. Ortiz Velasquez¹,⁶⁴
 J. Otwinowski¹,¹⁰⁷ M. Oya,⁹² K. Oyama¹,⁷⁶ Y. Pachmayer¹,⁹⁴ S. Padhan¹,⁴⁶ D. Pagano¹,^{131,54} G. Pać¹,⁶⁴
 A. Palasciano¹,⁴⁹ S. Panebianco¹,¹²⁸ H. Park¹,¹²³ H. Park¹,¹⁰⁴ J. Park¹,⁵⁷ J. E. Parkkila¹,³² R. N. Patra,⁹¹ B. Paul¹,²²
 H. Pei¹,⁶ T. Peitzmann¹,⁵⁸ X. Peng¹,⁶ M. Pennisi¹,²⁴ L. G. Pereira¹,⁶⁵ D. Peresunko¹,¹⁴⁰ G. M. Perez¹,⁷ S. Perrin¹,¹²⁸
 Y. Pestov,¹⁴⁰ V. Petráček¹,³⁵ V. Petrov¹,¹⁴⁰ M. Petrovici¹,⁴⁵ R. P. Pezzi¹,^{103,65} S. Piano¹,⁵⁶ M. Pikna¹,¹² P. Pillot¹,¹⁰³
 O. Pinazza¹,^{50,32} L. Pinsky,¹¹⁴ C. Pinto¹,⁹⁵ S. Pisano¹,⁴⁸ M. Płoskoń¹,⁷⁴ M. Planinic,⁸⁹ F. Pliquett,⁶³ M. G. Poghosyan¹,⁸⁷
 B. Polichtchouk¹,¹⁴⁰ S. Politano¹,²⁹ N. Poljak¹,⁸⁹ A. Pop¹,⁴⁵ S. Porteboeuf-Houssais¹,¹²⁵ V. Pozdniakov¹,¹⁴¹
 K. K. Pradhan¹,⁴⁷ S. K. Prasad¹,⁴ S. Prasad¹,⁴⁷ R. Preghenella¹,⁵⁰ F. Prino¹,⁵⁵ C. A. Pruneau¹,¹³⁴ I. Pshenichnov¹,¹⁴⁰
 M. Puccio¹,³² S. Pucillo¹,²⁴ Z. Pugelova,¹⁰⁶ S. Qiu¹,⁸⁴ L. Quaglia¹,²⁴ R. E. Quishpe,¹¹⁴ S. Ragoni¹,^{14,100}
 A. Rakotozafindrabe¹,¹²⁸ L. Ramello¹,^{130,55} F. Rami¹,¹²⁷ S. A. R. Ramirez¹,⁴⁴ T. A. Rancien,⁷³ M. Rasa¹,²⁶
 S. S. Räsänen¹,⁴³ R. Rath¹,⁵⁰ M. P. Rauch¹,²⁰ I. Ravasenga¹,⁸⁴ K. F. Read¹,^{87,120} C. Reckziegel¹,¹¹²
 A. R. Redelbach¹,³⁸ K. Redlich¹,^{79,f} C. A. Reetz¹,⁹⁷ A. Rehman,²⁰ F. Reidt¹,³² H. A. Reme-Ness¹,³⁴ Z. Rescakova,³⁷
 K. Reygers¹,⁹⁴ A. Riabov¹,¹⁴⁰ V. Riabov¹,¹⁴⁰ R. Ricci¹,²⁸ M. Richter¹,¹⁹ A. A. Riedel¹,⁹⁵ W. Riegler¹,³² C. Ristea¹,⁶²
 M. Rodríguez Cahuantzi¹,⁴⁴ K. Røed¹,¹⁹ R. Rogalev¹,¹⁴⁰ E. Rogochaya¹,¹⁴¹ T. S. Rogoschinski¹,⁶³ D. Rohr¹,³²
 D. Röhrich¹,²⁰ P. F. Rojas,⁴⁴ S. Rojas Torres¹,³⁵ P. S. Rokita¹,¹³³ G. Romanenko¹,¹⁴¹ F. Ronchetti¹,⁴⁸ A. Rosano¹,^{30,52}
 E. D. Rosas,⁶⁴ K. Roslon¹,¹³³ A. Rossi¹,⁵³ A. Roy¹,⁴⁷ S. Roy¹,⁴⁶ N. Rubini¹,²⁵ O. V. Rueda¹,^{114,75} D. Ruggiano¹,¹³³
 R. Rui¹,²³ B. Rumyantsev,¹⁴¹ P. G. Russek¹,² R. Russo¹,⁸⁴ A. Rustamov¹,⁸¹ E. Ryabinkin¹,¹⁴⁰ Y. Ryabov¹,¹⁴⁰
 A. Rybicki¹,¹⁰⁷ H. Rytkonen¹,¹¹⁵ W. Rzesz¹,¹³³ O. A. M. Saarimaki¹,⁴³ R. Sadek¹,¹⁰³ S. Sadhu¹,³¹ S. Sadovsky¹,¹⁴⁰
 J. Saetre¹,²⁰ K. Šafařík¹,³⁵ S. K. Saha¹,⁴ S. Saha¹,⁸⁰ B. Sahoo¹,⁴⁶ R. Sahoo¹,⁴⁷ S. Sahoo¹,⁶⁰ D. Sahu¹,⁴⁷ P. K. Sahu¹,⁶⁰
 J. Saini¹,¹³² K. Sajdakova,³⁷ S. Sakai¹,¹²³ M. P. Salván¹,⁹⁷ S. Sambyal¹,⁹¹ I. Sanna¹,^{32,95} T. B. Saramela,¹¹⁰
 D. Sarkar¹,¹³⁴ N. Sarkar,¹³² P. Sarma¹,⁴¹ V. Sarritzu¹,²² V. M. Sarti¹,⁹⁵ M. H. P. Sas¹,¹³⁷ J. Schambach¹,⁸⁷
 H. S. Scheid¹,⁶³ C. Schiaua¹,⁴⁵ R. Schicker¹,⁹⁴ A. Schmah,⁹⁴ C. Schmidt¹,⁹⁷ H. R. Schmidt,⁹³ M. O. Schmidt¹,³²
 M. Schmidt,⁹³ N. V. Schmidt¹,⁸⁷ A. R. Schmier¹,¹²⁰ R. Schotter¹,¹²⁷ A. Schröter¹,³⁸ J. Schukraft¹,³² K. Schwarz,⁹⁷

- K. Schweda⁹⁷, G. Sciolli²⁵, E. Scomparin⁵⁵, J. E. Seger¹⁴, Y. Sekiguchi¹²², D. Sekihata¹²², I. Selyuzhenkov^{97,140}, S. Senyukov¹²⁷, J. J. Seo⁵⁷, D. Serebryakov¹⁴⁰, L. Šerkšnytė⁹⁵, A. Sevcenco⁶², T. J. Shaba⁶⁷, A. Shabetai¹⁰³, R. Shahoyan³², A. Shangaraev¹⁴⁰, A. Sharma⁹⁰, B. Sharma⁹¹, D. Sharma⁴⁶, H. Sharma¹⁰⁷, M. Sharma⁹¹, S. Sharma⁷⁶, S. Sharma⁹¹, U. Sharma⁹¹, A. Shatat⁷², O. Sheibani¹¹⁴, K. Shigaki⁹², M. Shimomura⁷⁷, J. Shin¹¹, S. Shirinkin¹⁴⁰, Q. Shou³⁹, Y. Sibirjak¹⁴⁰, S. Siddhanta⁵¹, T. Siemiaczuk⁷⁹, T. F. Silva¹¹⁰, D. Silvermyr⁷⁵, T. Simantathammakul¹⁰⁵, R. Simeonov³⁶, B. Singh⁹¹, B. Singh⁹⁵, R. Singh⁸⁰, R. Singh⁹¹, R. Singh⁴⁷, S. Singh¹⁵, V. K. Singh¹³², V. Singhal¹³², T. Sinha⁹⁹, B. Sitar¹², M. Sitta^{130,55}, T. B. Skaali¹⁹, G. Skorodumovs⁹⁴, M. Slupecki⁴³, N. Smirnov¹³⁷, R. J. M. Snellings⁵⁸, E. H. Solheim¹⁹, J. Song¹¹⁴, A. Songmoolnak¹⁰⁵, F. Soramel²⁷, R. Spijkers⁸⁴, I. Sputowska¹⁰⁷, J. Staa⁷⁵, J. Stachel⁹⁴, I. Stan⁶², P. J. Steffanic¹²⁰, S. F. Stiefelmaier⁹⁴, D. Stocco¹⁰³, I. Storehaug¹⁹, P. Stratmann¹³⁵, S. Strazzi²⁵, C. P. Stylianidis⁸⁴, A. A. P. Suaipe¹¹⁰, C. Suire⁷², M. Sukhanov¹⁴⁰, M. Suljic³², R. Sultanov¹⁴⁰, V. Sumberia⁹¹, S. Sumowidagdo⁸², S. Swain⁶⁰, I. Szarka¹², M. Szymkowski¹³³, S. F. Taghavi⁹⁵, G. Taillepied⁹⁷, J. Takahashi¹¹¹, G. J. Tambave²⁰, S. Tang^{125,6}, Z. Tang¹¹⁸, J. D. Tapia Takaki¹¹⁶, N. Tapus¹²⁴, L. A. Tarasovicova¹³⁵, M. G. Tarzila⁴⁵, G. F. Tassielli³¹, A. Tauro³², G. Tejeda Muñoz⁴⁴, A. Telesca³², L. Terlizzi²⁴, C. Terrevoli¹¹⁴, G. Tersimonov³, S. Thakur⁴, D. Thomas¹⁰⁸, A. Tikhonov¹⁴⁰, A. R. Timmins¹¹⁴, M. Tkacik¹⁰⁶, T. Tkacik¹⁰⁶, A. Toia⁶³, R. Tokumoto⁹², N. Topilskaya¹⁴⁰, M. Toppi⁴⁸, F. Torales-Acosta¹⁸, T. Tork⁷², A. G. Torres Ramos³¹, A. Trifirò^{30,52}, A. S. Triolo^{30,52}, S. Tripathy⁵⁰, T. Tripathy⁴⁶, S. Trogolo³², V. Trubnikov³, W. H. Trzaska¹¹⁵, T. P. Trzcinski¹³³, A. Tumkin¹⁴⁰, R. Turrisi⁵³, T. S. Tveter¹⁹, K. Ullaland²⁰, B. Ulukutlu⁹⁵, A. Uras¹²⁶, M. Urioni^{54,131}, G. L. Usai²², M. Vala³⁷, N. Valle²¹, L. V. R. van Doremale⁵⁸, M. van Leeuwen⁸⁴, C. A. van Veen⁹⁴, R. J. G. van Weelden⁸⁴, P. Vande Vyvre³², D. Varga¹³⁶, Z. Varga¹³⁶, M. Vasileiou⁷⁸, A. Vasiliev¹⁴⁰, O. Vázquez Doce⁴⁸, V. Vechernin¹⁴⁰, E. Vercellin²⁴, S. Vergara Limón⁴⁴, L. Vermunt⁹⁷, R. Vértesi¹³⁶, M. Verweij⁵⁸, L. Vickovic³³, Z. Vilakazi¹²¹, O. Villalobos Baillie¹⁰⁰, A. Villani²³, G. Vino⁴⁹, A. Vinogradov¹⁴⁰, T. Virgili²⁸, V. Vislavicius⁷⁵, A. Vodopyanov¹⁴¹, B. Volkel³², M. A. Völkl⁹⁴, K. Voloshin¹⁴⁰, S. A. Voloshin¹³⁴, G. Volpe³¹, B. von Haller³², I. Vorobyev⁹⁵, N. Vozniuk¹⁴⁰, J. Vrláková³⁷, C. Wang³⁹, D. Wang³⁹, Y. Wang³⁹, A. Wegrzynek³², F. T. Weiglhofer³⁸, S. C. Wenzel³², J. P. Wessels¹³⁵, S. L. Weyhmiller¹³⁷, J. Wiechula⁶³, J. Wikne¹⁹, G. Wilk⁷⁹, J. Wilkinson⁹⁷, G. A. Willems¹³⁵, B. Windelband⁹⁴, M. Winn¹²⁸, J. R. Wright¹⁰⁸, W. Wu³⁹, Y. Wu¹¹⁸, R. Xu⁶, A. Yadav⁴², A. K. Yadav¹³², S. Yalcin⁷¹, Y. Yamaguchi⁹², S. Yang²⁰, S. Yano⁹², Z. Yin⁶, I.-K. Yoo¹⁶, J. H. Yoon⁵⁷, S. Yuan²⁰, A. Yuncu⁹⁴, V. Zacco²³, C. Zampolli³², F. Zanone⁹⁴, N. Zardoshti^{32,100}, A. Zarochentsev¹⁴⁰, P. Závada⁶¹, N. Zavyalov¹⁴⁰, M. Zhalov¹⁴⁰, B. Zhang⁶, L. Zhang³⁹, S. Zhang³⁹, X. Zhang⁶, Y. Zhang¹¹⁸, Z. Zhang⁶, M. Zhao¹⁰, V. Zherebchevskii¹⁴⁰, Y. Zhi¹⁰, D. Zhou⁶, Y. Zhou⁸³, J. Zhu^{6,97}, Y. Zhu⁶, S. C. Zugravel⁵⁵ and N. Zurlo^{131,54}

(ALICE Collaboration)

¹A.I. Alikhanyan National Science Laboratory (Yerevan Physics Institute) Foundation, Yerevan, Armenia²AGH University of Science and Technology, Cracow, Poland³Bogolyubov Institute for Theoretical Physics, National Academy of Sciences of Ukraine, Kiev, Ukraine⁴Bose Institute, Department of Physics and Centre for Astroparticle Physics and Space Science (CAPSS), Kolkata, India⁵California Polytechnic State University, San Luis Obispo, California, United States⁶Central China Normal University, Wuhan, China⁷Centro de Aplicaciones Tecnológicas y Desarrollo Nuclear (CEADEN), Havana, Cuba⁸Centro de Investigación y de Estudios Avanzados (CINVESTAV), Mexico City and Mérida, Mexico⁹Chicago State University, Chicago, Illinois, United States¹⁰China Institute of Atomic Energy, Beijing, China¹¹Chungbuk National University, Cheongju, Republic of Korea¹²Comenius University Bratislava, Faculty of Mathematics, Physics and Informatics, Bratislava, Slovak Republic¹³COMSATS University Islamabad, Islamabad, Pakistan¹⁴Creighton University, Omaha, Nebraska, United States¹⁵Department of Physics, Aligarh Muslim University, Aligarh, India¹⁶Department of Physics, Pusan National University, Pusan, Republic of Korea¹⁷Department of Physics, Sejong University, Seoul, Republic of Korea

- ¹⁸Department of Physics, University of California, Berkeley, California, United States
¹⁹Department of Physics, University of Oslo, Oslo, Norway
²⁰Department of Physics and Technology, University of Bergen, Bergen, Norway
²¹Dipartimento di Fisica, Università di Pavia, Pavia, Italy
²²Dipartimento di Fisica dell'Università and Sezione INFN, Cagliari, Italy
²³Dipartimento di Fisica dell'Università and Sezione INFN, Trieste, Italy
²⁴Dipartimento di Fisica dell'Università and Sezione INFN, Turin, Italy
²⁵Dipartimento di Fisica e Astronomia dell'Università and Sezione INFN, Bologna, Italy
²⁶Dipartimento di Fisica e Astronomia dell'Università and Sezione INFN, Catania, Italy
²⁷Dipartimento di Fisica e Astronomia dell'Università and Sezione INFN, Padova, Italy
²⁸Dipartimento di Fisica 'E.R. Caianiello' dell'Università and Gruppo Collegato INFN, Salerno, Italy
²⁹Dipartimento DISAT del Politecnico and Sezione INFN, Turin, Italy
³⁰Dipartimento di Scienze MIFT, Università di Messina, Messina, Italy
³¹Dipartimento Interateneo di Fisica 'M. Merlin' and Sezione INFN, Bari, Italy
³²European Organization for Nuclear Research (CERN), Geneva, Switzerland
³³Faculty of Electrical Engineering, Mechanical Engineering and Naval Architecture, University of Split, Split, Croatia
³⁴Faculty of Engineering and Science, Western Norway University of Applied Sciences, Bergen, Norway
³⁵Faculty of Nuclear Sciences and Physical Engineering, Czech Technical University in Prague, Prague, Czech Republic
³⁶Faculty of Physics, Sofia University, Sofia, Bulgaria
³⁷Faculty of Science, P.J. Šafárik University, Košice, Slovak Republic
³⁸Frankfurt Institute for Advanced Studies, Johann Wolfgang Goethe-Universität Frankfurt, Frankfurt, Germany
³⁹Fudan University, Shanghai, China
⁴⁰Gangneung-Wonju National University, Gangneung, Republic of Korea
⁴¹Gauhati University, Department of Physics, Guwahati, India
⁴²Helmholtz-Institut für Strahlen- und Kernphysik, Rheinische Friedrich-Wilhelms-Universität Bonn, Bonn, Germany
⁴³Helsinki Institute of Physics (HIP), Helsinki, Finland
⁴⁴High Energy Physics Group, Universidad Autónoma de Puebla, Puebla, Mexico
⁴⁵Horia Hulubei National Institute of Physics and Nuclear Engineering, Bucharest, Romania
⁴⁶Indian Institute of Technology Bombay (IIT), Mumbai, India
⁴⁷Indian Institute of Technology Indore, Indore, India
⁴⁸INFN, Laboratori Nazionali di Frascati, Frascati, Italy
⁴⁹INFN, Sezione di Bari, Bari, Italy
⁵⁰INFN, Sezione di Bologna, Bologna, Italy
⁵¹INFN, Sezione di Cagliari, Cagliari, Italy
⁵²INFN, Sezione di Catania, Catania, Italy
⁵³INFN, Sezione di Padova, Padova, Italy
⁵⁴INFN, Sezione di Pavia, Pavia, Italy
⁵⁵INFN, Sezione di Torino, Turin, Italy
⁵⁶INFN, Sezione di Trieste, Trieste, Italy
⁵⁷Inha University, Incheon, Republic of Korea
⁵⁸Institute for Gravitational and Subatomic Physics (GRASP), Utrecht University/Nikhef, Utrecht, Netherlands
⁵⁹Institute of Experimental Physics, Slovak Academy of Sciences, Košice, Slovak Republic
⁶⁰Institute of Physics, Homi Bhabha National Institute, Bhubaneswar, India
⁶¹Institute of Physics of the Czech Academy of Sciences, Prague, Czech Republic
⁶²Institute of Space Science (ISS), Bucharest, Romania
⁶³Institut für Kernphysik, Johann Wolfgang Goethe-Universität Frankfurt, Frankfurt, Germany
⁶⁴Instituto de Ciencias Nucleares, Universidad Nacional Autónoma de México, Mexico City, Mexico
⁶⁵Instituto de Física, Universidade Federal do Rio Grande do Sul (UFRGS), Porto Alegre, Brazil
⁶⁶Instituto de Física, Universidad Nacional Autónoma de México, Mexico City, Mexico
⁶⁷iThemba LABS, National Research Foundation, Somerset West, South Africa
⁶⁸Jeonbuk National University, Jeonju, Republic of Korea
⁶⁹Johann-Wolfgang-Goethe Universität Frankfurt Institut für Informatik, Fachbereich Informatik und Mathematik, Frankfurt, Germany
⁷⁰Korea Institute of Science and Technology Information, Daejeon, Republic of Korea
⁷¹KTO Karatay University, Konya, Turkey
⁷²Laboratoire de Physique des 2 Infinis, Irène Joliot-Curie, Orsay, France
⁷³Laboratoire de Physique Subatomique et de Cosmologie, Université Grenoble-Alpes, CNRS-IN2P3, Grenoble, France
⁷⁴Lawrence Berkeley National Laboratory, Berkeley, California, United States
⁷⁵Lund University Department of Physics, Division of Particle Physics, Lund, Sweden
⁷⁶Nagasaki Institute of Applied Science, Nagasaki, Japan
⁷⁷Nara Women's University (NWU), Nara, Japan

- ⁷⁸National and Kapodistrian University of Athens, School of Science, Department of Physics, Athens, Greece
⁷⁹National Centre for Nuclear Research, Warsaw, Poland
- ⁸⁰National Institute of Science Education and Research, Homi Bhabha National Institute, Jatni, India
⁸¹National Nuclear Research Center, Baku, Azerbaijan
- ⁸²National Research and Innovation Agency - BRIN, Jakarta, Indonesia
⁸³Niels Bohr Institute, University of Copenhagen, Copenhagen, Denmark
- ⁸⁴Nikhef, National institute for subatomic physics, Amsterdam, Netherlands
- ⁸⁵Nuclear Physics Group, STFC Daresbury Laboratory, Daresbury, United Kingdom
- ⁸⁶Nuclear Physics Institute of the Czech Academy of Sciences, Husinec-Řež, Czech Republic
⁸⁷Oak Ridge National Laboratory, Oak Ridge, Tennessee, United States
⁸⁸Ohio State University, Columbus, Ohio, United States
- ⁸⁹Physics department, Faculty of science, University of Zagreb, Zagreb, Croatia
⁹⁰Physics Department, Panjab University, Chandigarh, India
⁹¹Physics Department, University of Jammu, Jammu, India
- ⁹²Physics Program and International Institute for Sustainability with Knotted Chiral Meta Matter (SKCM2), Hiroshima University, Hiroshima, Japan
- ⁹³Physikalisches Institut, Eberhard-Karls-Universität Tübingen, Tübingen, Germany
⁹⁴Physikalisches Institut, Ruprecht-Karls-Universität Heidelberg, Heidelberg, Germany
⁹⁵Physik Department, Technische Universität München, Munich, Germany
⁹⁶Politecnico di Bari and Sezione INFN, Bari, Italy
- ⁹⁷Research Division and ExtreMe Matter Institute EMMI, GSI Helmholtzzentrum für Schwerionenforschung GmbH, Darmstadt, Germany
⁹⁸Saga University, Saga, Japan
- ⁹⁹Saha Institute of Nuclear Physics, Homi Bhabha National Institute, Kolkata, India
- ¹⁰⁰School of Physics and Astronomy, University of Birmingham, Birmingham, United Kingdom
- ¹⁰¹Sección Física, Departamento de Ciencias, Pontificia Universidad Católica del Perú, Lima, Peru
¹⁰²Stefan Meyer Institut für Subatomare Physik (SMI), Vienna, Austria
- ¹⁰³SUBATECH, IMT Atlantique, Nantes Université, CNRS-IN2P3, Nantes, France
¹⁰⁴Sungkyunkwan University, Suwon City, Republic of Korea
¹⁰⁵Suranaree University of Technology, Nakhon Ratchasima, Thailand
¹⁰⁶Technical University of Košice, Košice, Slovak Republic
- ¹⁰⁷The Henryk Niewodniczanski Institute of Nuclear Physics, Polish Academy of Sciences, Cracow, Poland
¹⁰⁸The University of Texas at Austin, Texas, United States
¹⁰⁹Universidad Autónoma de Sinaloa, Culiacán, Mexico
¹¹⁰Universidade de São Paulo (USP), São Paulo, Brazil
¹¹¹Universidade Estadual de Campinas (UNICAMP), Campinas, Brazil
¹¹²Universidade Federal do ABC, Santo André, Brazil
¹¹³University of Cape Town, Cape Town, South Africa
¹¹⁴University of Houston, Houston, Texas, United States
¹¹⁵University of Jyväskylä, Jyväskylä, Finland
¹¹⁶University of Kansas, Lawrence, Kansas, United States
¹¹⁷University of Liverpool, Liverpool, United Kingdom
¹¹⁸University of Science and Technology of China, Hefei, China
¹¹⁹University of South-Eastern Norway, Kongsberg, Norway
¹²⁰University of Tennessee, Knoxville, Tennessee, United States
¹²¹University of the Witwatersrand, Johannesburg, South Africa
¹²²University of Tokyo, Tokyo, Japan
¹²³University of Tsukuba, Tsukuba, Japan
¹²⁴University Politehnica of Bucharest, Bucharest, Romania
¹²⁵Université Clermont Auvergne, CNRS/IN2P3, LPC, Clermont-Ferrand, France
¹²⁶Université de Lyon, CNRS/IN2P3, Institut de Physique des 2 Infinis de Lyon, Lyon, France
¹²⁷Université de Strasbourg, CNRS, IPHC UMR 7178, F-67000 Strasbourg, France, Strasbourg, France
¹²⁸Université Paris-Saclay Centre d'Etudes de Saclay (CEA), IRFU, Département de Physique Nucléaire (DPhN), Saclay, France
¹²⁹Università degli Studi di Foggia, Foggia, Italy
¹³⁰Università del Piemonte Orientale, Vercelli, Italy
¹³¹Università di Brescia, Brescia, Italy
¹³²Variable Energy Cyclotron Centre, Homi Bhabha National Institute, Kolkata, India
¹³³Warsaw University of Technology, Warsaw, Poland
¹³⁴Wayne State University, Detroit, Michigan, United States
¹³⁵Westfälische Wilhelms-Universität Münster, Institut für Kernphysik, Münster, Germany

¹³⁶*Wigner Research Centre for Physics, Budapest, Hungary*¹³⁷*Yale University, New Haven, Connecticut, United States*¹³⁸*Yonsei University, Seoul, Republic of Korea*¹³⁹*Zentrum für Technologie und Transfer (ZTT), Worms, Germany*¹⁴⁰*Affiliated with an institute covered by a cooperation agreement with CERN*¹⁴¹*Affiliated with an international laboratory covered by a cooperation agreement with CERN*^aDeceased.^bAlso at: Max-Planck-Institut fur Physik, Munich, Germany.^cAlso at: Italian National Agency for New Technologies, Energy and Sustainable Economic Development (ENEA), Bologna, Italy.^dAlso at: Dipartimento DET del Politecnico di Torino, Turin, Italy.^eAlso at: Department of Applied Physics, Aligarh Muslim University, Aligarh, India.^fAlso at: Institute of Theoretical Physics, University of Wroclaw, Poland.^gAlso at: An institution covered by a cooperation agreement with CERN.